Check for updates

JIPB Journal of Integrative Plant Biology

Research Article
https://doi.org/10.1111/jipb.13264

MDP25 mediates the fine-tuning of microtubule organization in response to salt stress[oo]

Peizhi Yang[1], Jingwei Jin[1], Jingru Zhang[1], Dan Wang[1], Xuechun Bai[1], Wenfei Xie[1], Tianming Hu[1], Xuan Zhao[2,3], Tonglin Mao[4] and Tao Qin[1]*

1. College of Grassland Agriculture, Northwest A&F University, Yangling 712100, China
2. Research Center of Chinese Jujube, Hebei Agricultural University, Baoding 071001, China
3. College of Horticulture, Hebei Agricultural University, Baoding 071001, China
4. State Key Laboratory of Plant Physiology and Biochemistry, Department of Plant Sciences, College of Biological Sciences, China Agricultural University, Beijing 100193, China

*Correspondence: Tao Qin (tao.qin@nwafu.edu.cn)



Peizhi Yang



Tao Qin

ABSTRACT

Microtubules are dynamic cytoskeleton structures playing fundamental roles in plant responses to salt stress. The precise mechanisms by which microtubule organization is regulated under salt stress are largely unknown. Here, we report that *Arabidopsis thaliana* MICROTUBULE-DESTABILIZING PROTEIN 25 (MDP25; also known as PLASMA MEMBRANE-ASSOCIATED CATION-BINDING PROTEIN 1 (PCaP1)) helps regulate microtubule organization. Under salt treatment, elevated cytosolic Ca^{2+} concentration caused MDP25 to partially dissociate from the plasma membrane, promoting microtubule depolymerization. When Ca^{2+} signaling was blocked by BAPTA-AM or $LaCl_3$, microtubule depolymerization in wild-type and *MDP25*-overexpressing cells was slower, while there was no obvious change in *mdp25* cells. Knockout of *MDP25* improved microtubule reassembly and was conducive to microtubule integrity under long-term salt treatment and microtubule recovery after salt stress. Moreover, *mdp25* seedlings exhibited a higher survival rate under salt stress. The presence microtubule-disrupting reagent oryzalin or microtubule-stabilizing reagent paclitaxel differentially affected the survival rates of different genotypes under salt stress. MDP25 promoted microtubule instability by affecting the catastrophe and rescue frequencies, shrinkage rate and time in pause phase at the microtubule plus-end and the depolymerization rate at the microtubule minus-end. These findings reveal a role for MDP25 in regulating microtubule organization under salt treatment by affecting microtubule dynamics.

Keywords: calcium, MDP25, microtubule, salt stress

Yang, P., Jin, J., Zhang, J., Wang, D., Bai, X., Xie, W., Hu, T., Zhao, X., Mao, T., and Qin, T. (2022). MDP25 mediates the fine-tuning of microtubule organization in response to salt stress. J. Integr. Plant Biol. **64:** 1181–1195.

INTRODUCTION

Plants have developed adaptation strategies to mitigate the negative effect of salt stress on their growth and reproduction (Deinlein et al., 2014; Yang and Guo, 2018; Yu et al., 2020). Microtubules are dynamic cytoskeleton structures that participate in plant cell growth, morphogenesis, and responses to environmental signals including gravity, low temperature, mechanical forces, and salt stress (Landrein and Hamant, 2013; Nick, 2013; Sampathkumar et al., 2014; Zhang and Zhang, 2016; Zhou et al., 2017). Microtubule networks can rapidly alter their organization in response to salt stress, which is considered vital for plant growth and adaptation. For instance, cytosolic salt

© 2022 The Authors. *Journal of Integrative Plant Biology* published by John Wiley & Sons Australia, Ltd on behalf of Institute of Botany, Chinese Academy of Sciences.
This is an open access article under the terms of the Creative Commons Attribution-NonCommercial License, which permits use, distribution and reproduction in any medium, provided the original work is properly cited and is not used for commercial purposes.

imbalance results in microtubule depolymerization and salt sensitivity in *Arabidopsis sos1* mutant (Shoji et al., 2006). In addition, loss of function of *Arabidopsis* PREFOLDIN SUBUNIT 3 (PFD3) and PFD5 leads to a reduction in α- and β-tubulin as well as hypersensitivity to salt (Rodriguez-Milla and Salinas, 2009). When exposed to salt, cortical microtubules in plant cells undergo biphasic reorganization, including rapid microtubule depolymerization followed by reassembly of new microtubule networks (Dou et al., 2018; Wang and Mao, 2019). Both of these biphasic processes are essential for plant survival under high-salinity conditions (Li et al., 2017; Angelini et al., 2018; Yang et al., 2019).

Microtubule-associated proteins (MAPs), which regulate microtubule dynamics, stability, and organization, are key regulatory molecules in mediating cytoskeleton reorganization in response to salt stress (Buschmann and Lloyd, 2008; Sedbrook and Kaloriti, 2008; Dou et al., 2021). Under salt stress, the degradation of SPIRAL1 (SPR1), an *Arabidopsis* microtubule-stabilizing protein, by the 26S proteasome is accelerated, promoting the depolymerization of microtubules and favoring seedling survival (Wang et al., 2011). In addition, the salt stress-activated phospholipase D drives the production of phosphatidic acid (PA), which directly binds to MAP65-1 in *Arabidopsis* and enhances its microtubule-stabilizing activity, facilitating cortical microtubule reassembly and improving salt tolerance (Zhang et al., 2012). *Arabidopsis* COMPANION OF CELLULOSE SYNTHASE1 (CC1) and CC2, which enable microtubule polymerization and bundling, also facilitate microtubule reassembly under salt stress (Endler et al., 2015; Kesten et al., 2019). The Rho-related GTPase (ROP)-interactive Cdc42/Rac interactive binding (CRIB) motif-containing protein1 (RIC1) plays a negative role in microtubule reassembly. Under salt stress, *Arabidopsis* ROP2 is activated and drives RIC1 relocation to the plasma membrane, which dissipates the negative effect of RIC1 on microtubule and favors microtubule reassembly and plant survival (Li et al., 2017). WAVEDAMPENED2-LIKE5 (WDL5), an *Arabidopsis* microtubule stabilizer, is involved in the response of ethylene-mediated microtubule reassembly to salt stress. The alteration of WDL5 transcriptional levels by ETHYLENE-INSENSITIVE 3 (EIN3) results in abnormal microtubule reassembly (Dou et al., 2018). These studies demonstrate that MAPs affect the biphasic reorganization of microtubules. However, the precise regulatory mechanisms of microtubule organization under salt stress are still unclear.

MICROTUBULE-DESTABILIZING PROTEIN 25 (MDP25) is a hydrophilic cation-binding protein of the plant-specific developmentally regulated plasma membrane polypeptide (DREPP) family (Gantet et al., 1996). MDP25 is stably associated with the plasma membrane via *N*-myristoylation and an N-terminal polybasic cluster that binds to phosphatidylinositol phosphates (PtdInsPs) in the plasma membrane (Nagasaki et al., 2008; Kato et al., 2010; Vosolsobe et al., 2017). Deletion of the 25 N-terminal amino acids results in cytosolic accumulation of the protein (Nagata et al., 2016). MDP25 can bind to Ca^{2+}, and increased Ca^{2+} levels cause MDP25 to partially dissociate from the plasma membrane and move into the cytoplasm (Ide et al., 2007; Nagasaki et al., 2008; Li et al., 2011; Nagata et al., 2016). *In vitro*, MDP25 directly binds to and enhances microtubule depolymerization, and the microtubule-destabilizing activity of MDP25 is enhanced by Ca^{2+} (Li et al., 2011; Qin et al., 2012). In hypocotyl cells, MDP25 inhibits cell elongation by destabilizing cortical microtubules in response to the Ca^{2+} signal stimulated by light (Li et al., 2011). MDP25 is similarly hypothesized to regulate stomatal closure, root hydrotropic response, and immunity responses via its effects on microtubules (Nagata et al., 2016; Tanaka-Takada et al., 2019; Giovannoni et al., 2021). The homologs of MDP25 in rice and *Medicago truncatula* are also MAPs. OsDREPP2 shows affinity to microtubules and inhibits microtubule polymerization *in vitro* (Yamada et al., 2015), and MtDREPP triggers fragmentation of microtubules in membrane nanodomains during rhizobial infections (Su et al., 2020). These studies demonstrate that MDP25 is an important microtubule regulatory protein in response to the cytoplasmic Ca^{2+} signal.

In this study, we focused on the functional mechanisms by which MDP25 regulates plant response to salt stress. By observing the subcellular localization of MDP25 and exploring its effect on the biphasic reorganization of microtubules and *Arabidopsis* survival under salt stress, we observed that MDP25 partially dissociated from the plasma membrane in response to elevated cytosolic Ca^{2+} concentration and regulated microtubule reorganization under salt stress by affecting the dynamics of individual microtubules, such as: catastrophe and rescue frequencies; shrinkage rate and time in pause phase at the microtubule plus-end; and depolymerization rate at the microtubule minus-end. Knockout of *MDP25* delayed the depolymerization of microtubules, but promoted the subsequent reassembly process and plant survival under salt treatment. Taken together, our results uncover a mechanism whereby MDP25 decodes the Ca^{2+} signal stimulated by salt stress and regulates microtubule organization under salt treatment by affecting the dynamics of individual microtubules at both the plus- and minus-ends, which establishes a connection between the core salt signaling pathway and microtubule organization.

RESULTS

The expression and localization of MDP25 are regulated by salt stress

To determine whether *MDP25* plays a role in plant response to salt stress, the expression of *MDP25* under salt stress was investigated. Seven-d-old P_{MDP25}:*GUS Arabidopsis* transgenic seedlings previously described were immersed in 1/2 Murashige–Skoog (MS) solution with 175 mmol/L NaCl for 0, 6, 12, 18, 24, or 30 h, respectively (Li et al., 2011). The β-glucuronidase (GUS) signal first decreased after exposure to salt for 6 h, then increased and peaked at 18 h after exposure to salt, and finally returned to normal levels (Figure 1A). To further

17447909, 2022, 6, Downloaded from https://onlinelibrary.wiley.com/doi/10.1111/jipb.13264 by Northwest Agri & Forestry, Wiley Online Library on [03/11/2026]. See the Terms and Conditions (https://onlinelibrary.wiley.com/terms-and-conditions) on Wiley Online Library for rules of use; OA articles are governed by the applicable Creative Commons License

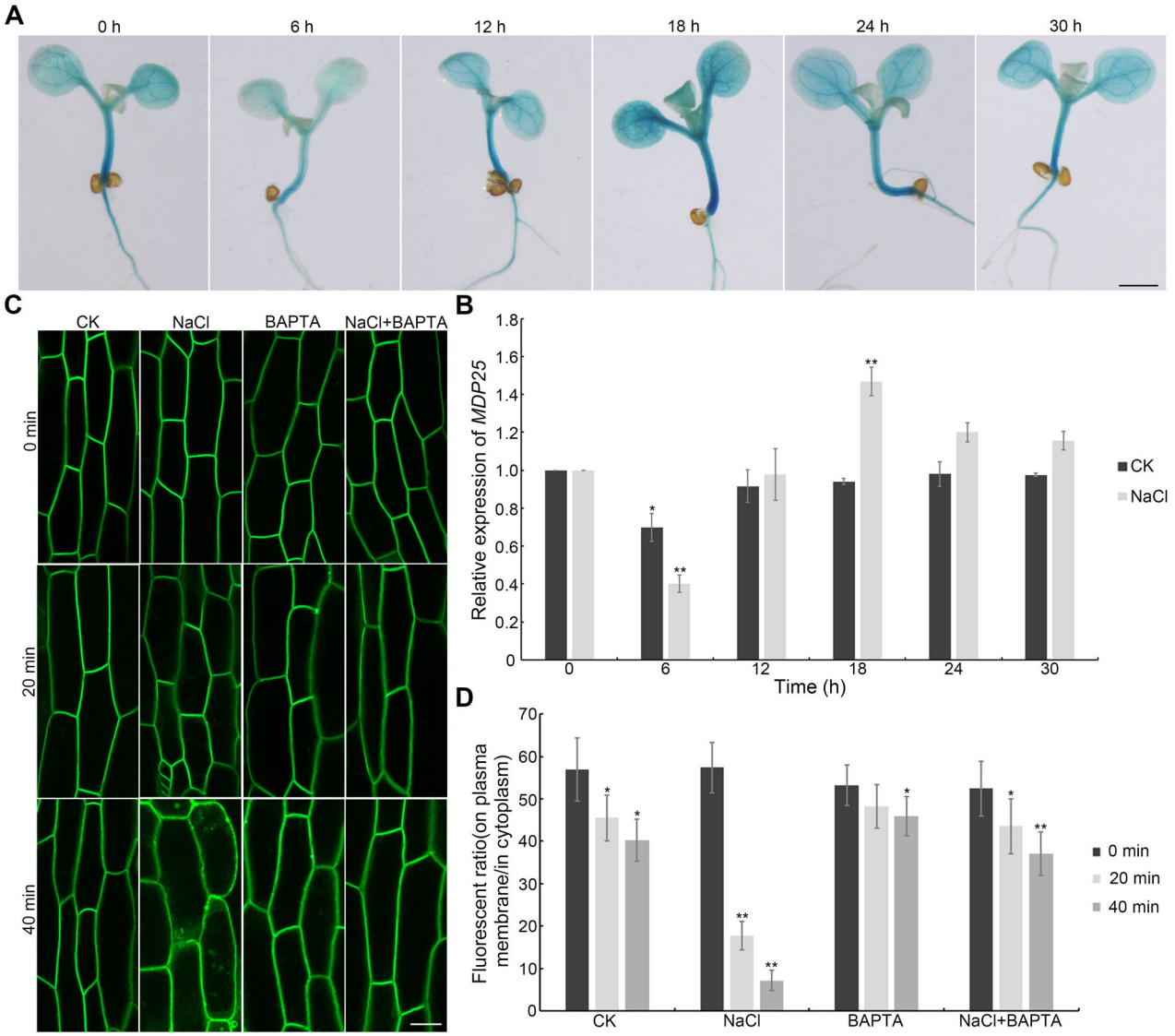


Figure 1. The expression and subcellular localization of MDP25 were subtly regulated under salt treatment

(**A**) P_{MDP25}:GUS activities in 7-d-old transgenic seedlings under 175 mmol/L NaCl treatment for the indicated times. Bar = 1 mm. (**B**) Relative transcript levels of *MDP25* under 175 mmol/L NaCl treatment for the indicated times measured by qPCR. $^{*}P < 0.05$ and $^{**}P < 0.01$ by *t*-test compared with the transcript levels at 0 h. Data represent means ± *SD*. (**C**) Subcellular localization of MDP25 in hypocotyl cells under 175 mmol/L NaCl treatment in the presence or absence of 300 μmol/L BAPTA-AM. Bar = 20 μm. (**D**) The ratio of fluorescent intensity on the plasma membrane to that in the cytoplasm. Fluorescent signals of more than 50 cells from 10 seedlings of each treatment were used for measurement. $^{*}P < 0.05$ and $^{**}P < 0.01$ by *t*-test compared with the fluorescent ratio at 0 min. Data represent means ± *SD*. CK, control conditions; GUS, β-glucuronidase; MDP25, MICROTUBULE-DESTABILIZING PROTEIN 25; qPCR, quantitative polymerase chain reaction.

investigate the regulation of *MDP25* expression by salt stress, we extracted total RNA from wild-type (WT) seedlings immersed in half-strength 1/2 MS solution with or without 175 mmol/L NaCl for 0, 6, 12, 18, 24, or 30 h. We determined expression levels of *MDP25* using reverse transcription quantitative polymerase chain reaction (qPCR). Consistent with the GUS activity analysis, the expression of *MDP25* was 60.1% lower in seedlings treated with NaCl for 6 h, but only 30.3% lower in seedlings in mock solution for 6 h, compared with the expression level at 0 h. Seedlings exposed to salt for longer periods had higher transcriptional levels; the expression level in seedlings treated with NaCl for 18 h was 1.47-fold that at 0 h, and there was no significant difference in transcript level between seedlings treated with mock solution for 0 h and those treated with mock solution for 18 h (Figure 1B). These results suggest that the accumulation of *MDP25* transcripts is subtly regulated in seedlings exposed to salt treatment.

Salt stress induces rapid elevation of cytosolic free Ca^{2+} concentration (Pan et al., 2012; Choi et al., 2014), which causes MDP25 to partially dissociate from the plasma membrane and move into the cytoplasm (Li et al., 2011). We investigated whether the subcellular localization of MDP25

17447909, 2022, 6, Downloaded from https://onlinelibrary.wiley.com/doi/10.1111/jipb.13264 by Northwest Agri & Forestry, Wiley Online Library on [03/11/2026]. See the Terms and Conditions (https://onlinelibrary.wiley.com/terms-and-conditions) on Wiley Online Library for rules of use; OA articles are governed by the applicable Creative Commons License

changes in seedlings exposed to salt. Five-d-old *35S:MDP25-GFP* transgenic seedlings grown on 1/2 MS medium plates were immersed in distilled water with or without 175 mmol/L NaCl for 0, 20, or 40 min, and the subcellular localization of MDP25 in epidermal cells of hypocotyls was visualized. MDP25 was mainly localized on the plasma membrane throughout the treatment under control conditions, although the ratio of fluorescent intensity on the plasma membrane to that in the cytoplasm decreased slightly with extended treatment time, probably attributable to the change of seedling growth conditions (Figure 1C, D). Nonetheless, the green fluorescent protein (GFP) signal of MDP25 on the plasma membrane was attenuated but that in the cytoplasm increased when seedlings were exposed to NaCl (Figure 1C). The ratio of fluorescent intensity on the plasma membrane to that in the cytoplasm decreased by 69.1% and 87.5% after salt treatment for 20 and 40 min, respectively, while that under control conditions decreased by 20.1% and 29.3% after 20 and 40 min, respectively, compared with that at 0 min (Figure 1D). These data suggest that salt stress may induce MDP25 to partially dissociate from the plasma membrane within 20 min.

To determine whether the rapid change in MDP25 localization under salt treatment is attributable to elevated cytosolic Ca^{2+} concentration, we pretreated *35S:MDP25-GFP* transgenic seedlings with 300 μmol/L of the Ca^{2+} chelator 1,2-bis(2-aminophenoxy)ethane-*N,N, N′,N′*-tetraacetic acid tetrakis (acetoxymethyl ester) (BAPTA-AM) for 30 min (Britigan et al., 1998) and then treated them with distilled water with or without 175 mmol/L NaCl in the presence of 300 μmol/L BAPTA-AM. Similar to that under treatment with distilled water alone, the ratio of fluorescent intensity on the plasma membrane to that in the cytoplasm under exposure to BAPTA-AM only slightly decreased with treatment time. The dissociation of MDP25 from the plasma membrane was greatly alleviated by BAPTA-AM under exposure to salt. The ratio of fluorescent intensity on the plasma membrane to that in the cytosol decreased by 16.9% and 29.4% after exposure to salt and BAPTA-AM for 20 and 40 min, respectively, compared with that at 0 min (Figure 1C, D). These data suggest that the dissociation of MDP25 from the plasma membrane is disrupted by blocking the increase of cytosolic Ca^{2+} concentration.

To further confirm the rapid change in MDP25 localization under salt treatment is attributable to elevated cytosolic Ca^{2+} concentration, we determined the subcellular localization of MDP25 and its Ca^{2+}-related site mutated variant, mMDP25, in the previously described transgenic lines P_{MDP25}*:MDP25-GFP/mdp25* and P_{MDP25}*:mMDP25-GFP/mdp25* following treatment with 175 mmol/L NaCl (Qin et al., 2014). The subcellular localization of MDP25 and mMDP25 was observed in epidermal cells at the bottom of hypocotyls, where the GFP signal was stronger and easily observed. MDP25 dissociated from the plasma membrane and moved into the cytosol after salt treatment for 40 min; the ratio of fluorescent intensity on the plasma membrane to that in the cytosol was 79.7% lower at 40 min compared with that at 0 min. However, the amount of mMDP25 dissociated from the plasma membrane was much smaller; the fluorescent ratio was only 28.9% lower at 40 min than at 0 min (Figure S1). These data demonstrate that MDP25 decodes the salt stress-stimulated Ca^{2+} signal by changing its subcellular localization.

The reorganization and integrity of cortical microtubule array were regulated by MDP25 under salt treatment

Microtubules function in plant responses to salt stress (Zhou et al., 2017; Dou et al., 2018), and MDP25 is an important microtubule-destabilizing protein. Therefore, we hypothesized that MDP25 participates in the regulation of microtubule biphasic reorganization under salt stress. We tested this hypothesis with previously described WT, *mdp25*, and *35S:MDP25* overexpression (OE) lines with yellow fluorescent protein (YFP)-tubulin tags (Li et al., 2011). Five-d-old seedlings were immersed in 1/2 MS solution containing 175 mmol/L NaCl for 0, 0.5, 1, 2, 4, 8, 12, 18, 24, 32, or 48 h. We analyzed the cortical microtubules in epidermal cells from the hypocotyl upper region and observed that they were partially depolymerized within 0.5 h of salt treatment. The microtubule density in all genotypes decreased notably after exposure to salt; 175 mmol/L NaCl resulted in the depolymerization of most cortical microtubules within 4 h (Figure 2A).

The deficiency of *MDP25* in *mdp25* mutant seedlings disrupted the depolymerization of microtubules, whereas the OE of *MDP25* in OE seedlings facilitated this process. After exposure to salt for 0.5, 1, and 2 h, the density of microtubules (the number of microtubules across a fixed 10-μm line vertical to the orientation of most cortical microtubules) decreased slower in *mdp25* cells and faster in OE cells than that in WT cells. The microtubule density in WT cells decreased by 31.3%, 56.2%, and 70.0%, respectively, whereas that in *mdp25* cells decreased by 15.4%, 23.5%, and 66.5%, respectively, and that in OE cells decreased by 35.2%, 62.4%, and 84.6%, respectively (Figure 2B). Considering that MDP25 partially dissociates from the plasma membrane within 20 min under salt treatment (Figure 1C, D), and that Ca^{2+} enhances the microtubule-destabilizing activity of MDP25 (Qin et al., 2012), it is likely that the Ca^{2+} signal induced by salt stress regulates the effect of MDP25 on microtubules, causing it to partially dissociate from the plasma membrane and enhancing its microtubule-destabilizing activity.

To test this hypothesis, 5-d-old WT, *mdp25*, and OE seedlings with YFP-tubulin tags were pretreated with 300 μmol/L BAPTA-AM for 30 min and then treated with 175 mmol/L NaCl in the presence of 300 μmol/L BAPTA-AM for 0, 1, 2, or 4 h. The depolymerization of microtubules in WT and OE seedlings was much slower, whereas there was no obvious change in *mdp25* seedlings, when Ca^{2+} signaling was blocked by BAPTA-AM (Figure 2C). That is, when

17447909, 2022, 6, Downloaded from https://onlinelibrary.wiley.com/doi/10.1111/jipb.13264 by Northwest Agri & Forestry, Wiley Online Library on [03/11/2026]. See the Terms and Conditions (https://onlinelibrary.wiley.com/terms-and-conditions) on Wiley Online Library for rules of use; OA articles are governed by the applicable Creative Commons License

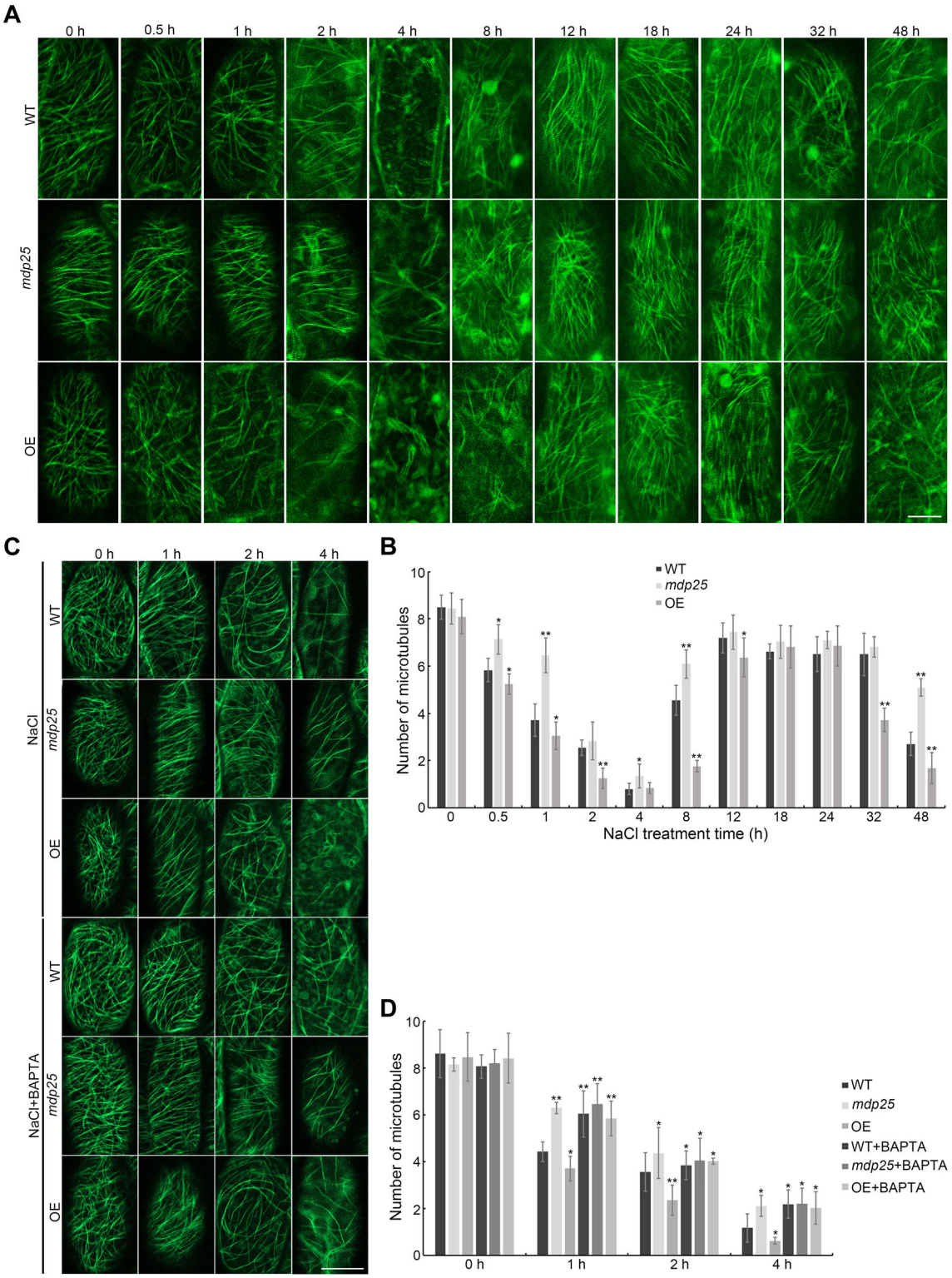


Figure 2. MDP25 regulates the biphasic reorganization of microtubules under salt stress

(**A**) Cortical microtubules in hypocotyl epidermal cells from wild-type (WT), *mdp25*, or *MDP25*-overexpressing (OE) seedlings under 175 mmol/L NaCl treatment for the indicated times. Bar = 10 μm. (**B**) Quantification of cortical microtubules ($n > 20$ cells for each sample). $^*P < 0.05$ and $^{**}P < 0.01$ by *t*-test comparing the number of cortical microtubules in *mdp25* or OE cells with that in WT cells under the same conditions. Data represent means ± *SD*. (**C**) Cortical microtubules in hypocotyl epidermal cells from seedlings of each genotype under 175 mmol/L NaCl treatment in the presence or absence of 300 μmol/L BAPTA-AM for the indicated times. Bar = 20 μm. (**D**) Quantification of cortical microtubules ($n > 20$ cells for each sample). $^*P < 0.05$ and $^{**}P < 0.01$ by *t*-test comparing the number of cortical microtubules with that in WT cells treated with NaCl alone under the same time point. Data represent means ± *SD*. MDP25, MICROTUBULE-DESTABILIZING PROTEIN 25.

17447909, 2022, 6, Downloaded from https://onlinelibrary.wiley.com/doi/10.1111/jipb.13264 by Northwest Agri & Forestry, Wiley Online Library on [03/11/2026]. See the Terms and Conditions (https://onlinelibrary.wiley.com/terms-and-conditions) on Wiley Online Library for rules of use; OA articles are governed by the applicable Creative Commons License

seedlings were treated with NaCl alone for 1, 2, or 4 h, the density of microtubules decreased by 48.7%, 58.8%, or 86.4% in WT cells and by 56.2%, 72.1%, or 92.7% in OE cells but only by 22.7%, 46.3%, or 74.1% in *mdp25* cells, respectively, compared with that at 0 h (Figure 2D). However, when treated with NaCl for 1, 2, or 4 h in the presence of BAPTA-AM, the density of microtubules decreased by 25.1%, 52.3%, or 72.8% in WT cells; by 30.4%, 52.2%, or 76.0% in OE cells; and, similarly, by 21.1%, 50.1%, or 73.1% in *mdp25* cells, respectively, compared with that at 0 h (Figure 2D). These data suggest that MDP25 decodes the Ca^{2+} signal stimulated by salt stress and regulates the depolymerization of microtubules.

To further confirm this conclusion, we also disrupted Ca^{2+} signaling by pretreating seedlings with 2 μmol/L lanthanum chloride ($LaCl_3$), a calcium-channel blocker, for 30 min (Liao et al., 2017). $LaCl_3$ slowed the depolymerization of microtubules in WT and OE cells (Figure S2A). The density of microtubules in WT cells decreased by 50.6%, 64.8%, or 77.8% when treated with NaCl alone for 1, 2, or 4 h, respectively, but only decreased by 36.5%, 51.2%, and 65.1%, respectively, in the presence of $LaCl_3$ compared with that at 0 h (Figure S2B). A similar pattern was observed in OE cells when $LaCl_3$ was applied (Figure S2). These data demonstrate that the Ca^{2+} signal stimulated by salt stress plays a role in microtubule depolymerization via MDP25.

When analyzing the reassembly of microtubules, we observed that a greater proportion of microtubules reassembled in *mdp25* than in WT cells after 8 h of NaCl treatment, whereas the microtubule array in OE cells only slightly recovered. The density of microtubules in WT and *mdp25* cells recovered to peak levels after exposure to salt for 12 h, whereas that in OE cells recovered after 18 h (Figure 2A, B). The density of microtubules remained at peak levels during subsequent observations at 18 and 24 h after exposure to salt. However, after 32 h of salt exposure, the recovered microtubule array in OE cells was partially depolymerized and that in WT and *mdp25* cells was slightly depolymerized. After exposure to salt for 48 h, most microtubules in OE cells were depolymerized, but a large proportion of microtubules in *mdp25* cells remained (Figure 2A). At 48 h, the microtubule densities in WT, *mdp25*, and OE cells were 31.9%, 60.4%, and 20.8% of that in untreated cells, respectively (Figure 2B). These data demonstrate that artificially maintaining higher expression levels of *MDP25* in OE cells is unfavorable for maintaining the stability of reorganized microtubules under long-term salt stress.

To investigate the recovery of the depolymerized microtubule organization after the removal of salt stress, seedlings with YFP-tubulin tags grown on 1/2 MS medium plates were transferred onto 1/2 MS medium plates supplemented with 200 mmol/L NaCl for 3 d. Treated seedlings were transferred back onto 1/2 MS medium plates for cortical microtubule recovery. When treated with 200 mmol/L NaCl for 2 d, microtubules in seedlings of all genotypes were sparser than those in untreated seedlings. However, there were more microtubules in *mdp25* and fewer microtubules in OE than in WT cells. When the treatment was prolonged for 3 d, most microtubules in WT and OE cells were depolymerized but a larger proportion of microtubules remained in *mdp25* cells (Figures 3 and S3).

Consistent with a previous study in which microtubule organization severely disrupted by salt stress recovered well after the removal of salt stress (Zhang et al., 2012), microtubules were reassembled in WT and *mdp25* cells after removing salt stress (Figures 3 and S3). When microtubules recovered for 2 d, the density of microtubules in *mdp25* cells recovered to levels similar to those in seedlings before treatment. The microtubule density in WT pavement cells also recovered to normal levels, whereas microtubules in OE cells were still recovering, and the microtubule density was much lower than that in seedlings before treatment (Figures 3 and S3). Intriguingly, it is likely that the morphology of most OE pavement cells could not be maintained after salt treatment for 3 d; this abnormal cell morphology still did not recover after the removal of salt stress for 2 d (Figure S3A).

To further explore the morphological change in OE pavement cells under salt conditions, we stained the pavement cells with propidium iodide. Both WT and OE pavement cell morphology became abnormal after seedlings were transferred onto 200 mmol/L NaCl medium plates for 3 d. Furthermore, MDP25 OE pavement cells showed obvious plasmolysis (Figure S4). These data demonstrate that decreased *MDP25* expression facilitates the recovery of microtubule organization after the removal of salt stress.

MDP25 affects plant seedling survival under salt stress

High-salinity conditions induce rapid hyperosmotic stress and slow ionic stress, causing premature senescence and potential plant death. To explore the effect of MDP25 on survival under salt treatment, seedlings of 4-d-old WT, *mdp25*, and two MDP25-overexpressing representative lines (OE #1 and OE #2) grown on 1/2 MS medium plates were transferred onto 1/2 MS plates supplemented with 0, 150, or 175 mmol/L NaCl. Seven d later, more OE seedlings were dead, but a lower proportion of *mdp25* seedlings became bleached compared with WT seedlings (Figure 4A). While 17.7% of OE #1 and 10.0% of OE #2 seedlings died, only 5.3% of WT and 0.3% of *mdp25* seedlings were bleached under 150 mmol/L NaCl treatment. Under 175 mmol/L NaCl treatment, the percentages of dead WT and *mdp25* seedlings were 30.2% and 16.5%, respectively, whereas more than 42% of OE line seedlings were dead (Figure 4B). These findings suggest that knockout of *MDP25* is favorable for seedling survival under salt treatment. To further test this conclusion, the role of MDP25 in salt tolerance of plants grown in soil was evaluated. Four-week-old WT, *mdp25*, and OE seedlings in soil were irrigated with 175 mmol/L NaCl. Eight d later, damage to leaves was observed. A higher proportion of OE leaves and fewer *mdp25* leaves were bleached relative to WT leaves. Fifteen d later, all WT and

17447909, 2022, 6, Downloaded from https://onlinelibrary.wiley.com/doi/10.1111/jipb.13264 by Northwest Agri & Forestry, Wiley Online Library on [03/11/2026]. See the Terms and Conditions (https://onlinelibrary.wiley.com/terms-and-conditions) on Wiley Online Library for rules of use; OA articles are governed by the applicable Creative Commons License

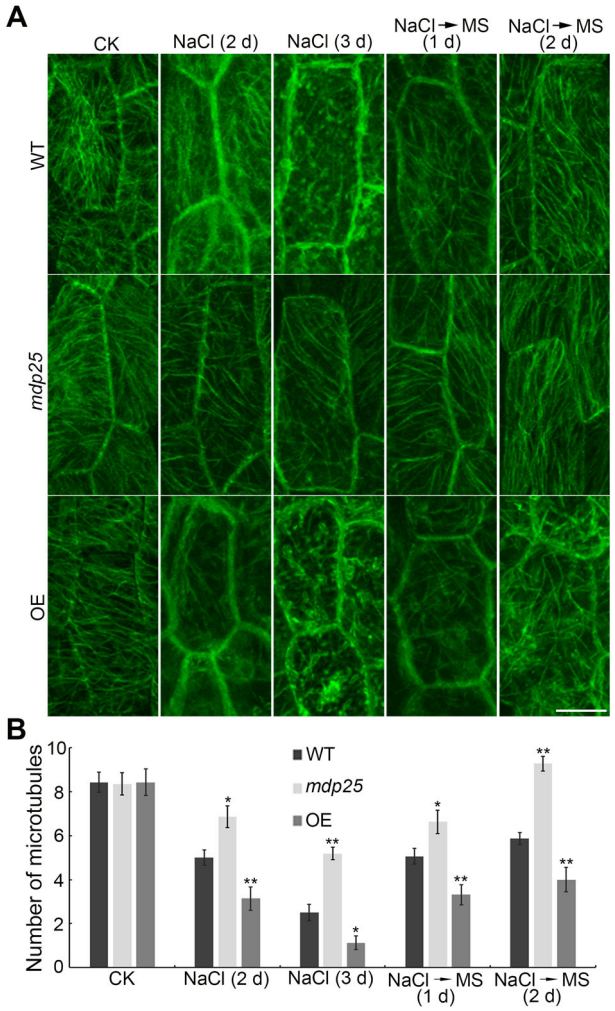


Figure 3. MDP25 affects the recovery of depolymerized microtubules in hypocotyl cells after the removal of salt stress

(**A**) The recovery of depolymerized cortical microtubules in hypocotyl cells from wild-type (WT), *mdp25*, or *MDP25*-overexpressing (OE) seedlings after removing salt stress. Bars = 20 μm. (**B**) Quantification of cortical microtubules ($n > 20$ cells for each sample). $^{*}P < 0.05$ and $^{**}P < 0.01$ by *t*-test comparing the number of cortical microtubules in *mdp25* or OE cells with that in WT cells under the same conditions. Data represent means ± *SD*. MDP25, MICROTUBULE-DESTABILIZING PROTEIN 25

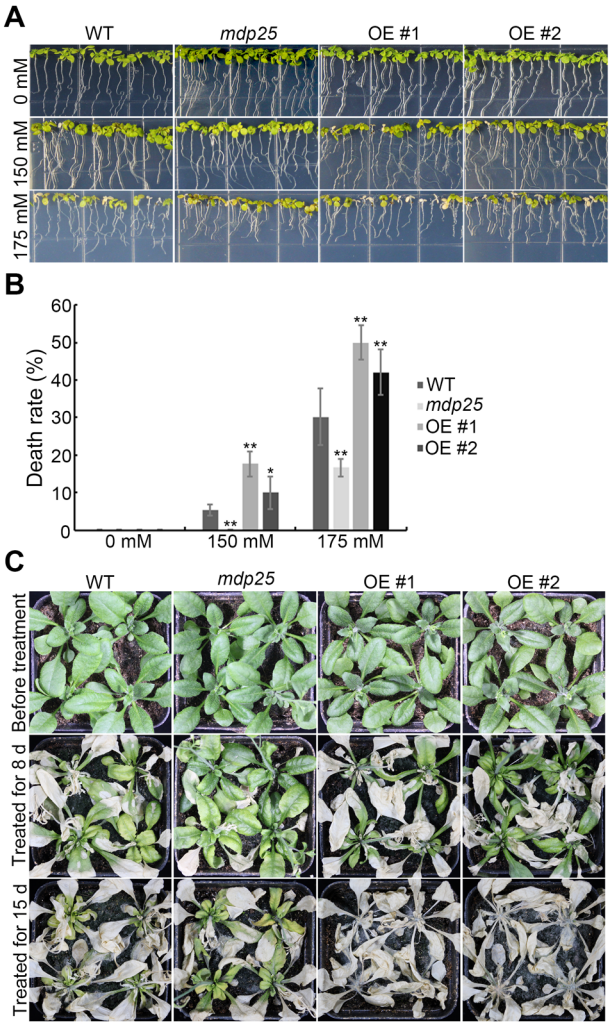


Figure 4. MDP25 affects plant survival under salt stress

(**A**) Representative images of wild-type (WT), *mdp25*, and overexpression (OE) seedlings grown on medium plates with the indicated concentrations of NaCl for 7 d. (**B**) The proportion of dead seedlings. At least 100 seedlings of each genotype were counted. $^{*}P < 0.05$ and $^{**}P < 0.01$ by *t*-test compared with the WT. Data represent means ± *SD*. (**C**) Morphology of soil-grown seedlings under salt stress. Four-week-old seedlings irrigated with 175 mmol/L NaCl. Photographs were taken before and after salt treatment for 8 and 15 d. MDP25, MICROTUBULE-DESTABILIZING PROTEIN 25.

mdp25 leaves showed chlorosis or bleaching, but no seedlings died; however, nearly all OE seedlings had died (Figure 4C).

To further test whether the phenotype of *mdp25* under salt stress is attributable to the loss of MDP25, we randomly selected two transgenic lines (P_{MDP25}:*MDP25*/*mdp25* #1 and P_{MDP25}:*MDP25*/*mdp25* #2) with similar expression levels of *MDP25* to that in the WT to perform complementary analysis (Figure S5A). More WT and P_{MDP25}:*MDP25*/*mdp25* transgenic seedlings died than *mdp25* seedlings did after exposure to NaCl for 7 d (Figure S5B). In the presence of 150 mmol/L NaCl, only 1.7% of *mdp25* seedlings died, whereas mortality rates of P_{MDP25}:*MDP25*/*mdp25* transgenic lines were 10.0% and 8.8%. When the concentration of NaCl was 175 mmol/L, approximately 22.6% of *mdp25* seedlings were bleached, but more than 36.3% of WT and P_{MDP25}:*MDP25*/*mdp25* transgenic seedlings died (Figure S5C). The tolerant phenotype of *mdp25* seedlings in soil was also compromised by P_{MDP25}:*MDP25*. After NaCl irrigation, the leaf chlorosis and bleaching of WT and P_{MDP25}:*MDP25*/*mdp25* transgenic seedlings was more severe than that of *mdp25* seedlings (Figure S5D). These data demonstrate that MDP25 participates in plant adaptation to salt stress.

To evaluate the association between MDP25 microtubule regulatory function and the plant phenotype under salt stress, 4-d-old WT, *mdp25*, and OE seedlings were transferred onto 1/2 MS plates supplemented with 175 mmol/L NaCl alone or

17447909, 2022, 6, Downloaded from https://onlinelibrary.wiley.com/doi/10.1111/jipb.13264 by Northwest Agri & Forestry, Wiley Online Library on [03/11/2026]. See the Terms and Conditions (https://onlinelibrary.wiley.com/terms-and-conditions) on Wiley Online Library for rules of use; OA articles are governed by the applicable Creative Commons License

with 175 mmol/L NaCl and 0.5 μmol/L of the microtubule-disrupting reagent oryzalin or 2 μmol/L of the microtubule-stabilizing reagent paclitaxel (taxol). Oryzalin improved the survival of WT seedlings under salt stress; the proportion of dead WT seedlings decreased by nearly one-third with oryzalin compared to without oryzalin. However, the proportion of dead OE seedlings increased by 0.64-fold with oryzalin compared to without oryzalin. No significant change was observed in *mdp25* seedlings (Figure S6). When the salt medium was supplemented with 2 μmol/L taxol, a higher proportion of WT and *mdp25* seedlings became bleached compared to salt medium without taxol. Moreover, the proportion of WT and *mdp25* dead seedlings increased by 0.24-fold and 0.45-fold, respectively. However, the effect of taxol on OE was weaker; taxol treatment increased dead seedlings by 0.13-fold compared with no taxol treatment (Figure S6). These results suggest that the effect of MDP25 on microtubule organization is one of the mechanisms by which MDP25 regulates plant response to salt stress.

MDP25 can also regulate actin filaments (Qin et al., 2014). To evaluate whether MDP25-mediated actin dynamics are also responsible for the plant phenotype under salt treatment, 4-d-old WT, *mdp25* and OE seedlings were transferred onto 1/2 MS plates supplemented with 175 mmol/L NaCl and 0 or 10 nmol/L of the F-actin depolymerization reagent latrunculin B (LatB). LatB slightly enhanced the tolerance of WT seedlings to salt stress; the proportion of dead seedling decreased from 34.9% in the control treatment to 27.9% in the LatB treatment. However, the mortality of OE seedlings increased significantly; there were 1.23-fold more dead seedlings in the LatB medium than in the control medium. No significant differences were observed in *mdp25* seedling mortality under LatB treatment (Figure S7). These results suggest that MDP25-mediated actin dynamics are also related to MDP25 function under salt stress.

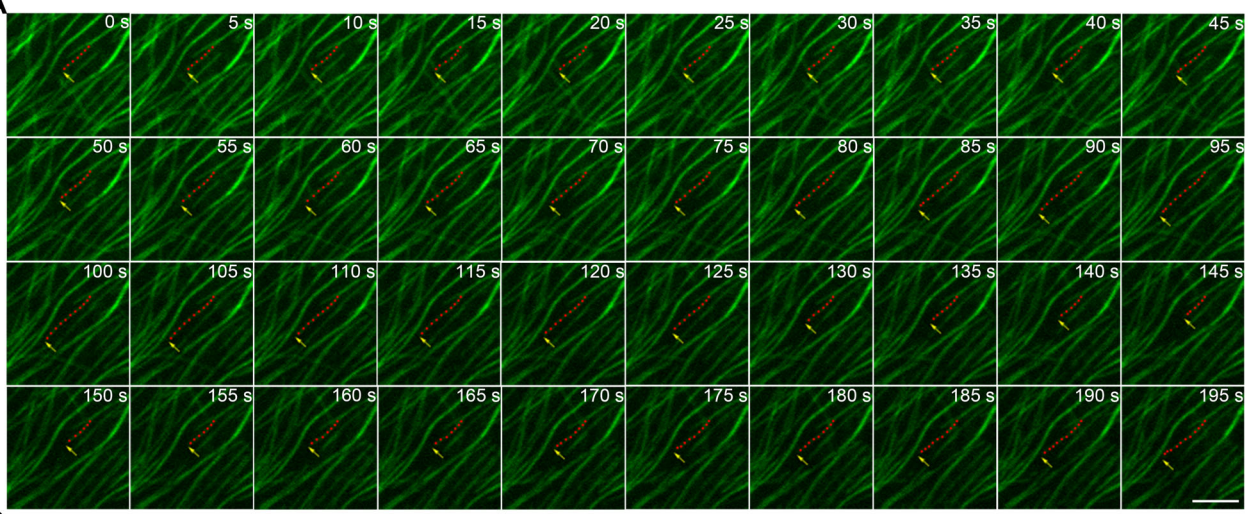
MDP25 affects microtubule dynamics under salt treatment

Microtubule organization is closely related to the dynamics of individual microtubules. Since MDP25 promoted microtubule depolymerization under salt treatment (Figure 2), we further analyzed microtubule dynamics under salt treatment using confocal time-lapse imaging. Five-d-old WT, *mdp25*, and OE seedlings with YFP-tubulin tags were immersed in 1/2 MS solution with or without 150 mmol/L NaCl for 1 h. Microtubules with a clearly visible leading plus-end in hypocotyl cells were analyzed (Figure 5A). The results showed that microtubule dynamics were altered in *mdp25* and OE hypocotyl cells compared with those in WT cells. Under control conditions, catastrophe and rescue frequencies of individual microtubules were lower in *mdp25* cells (49.5% and 89.6% of that in WT cells, respectively) but slightly higher in OE cells (119.1% and 104.6% of that in WT cells, respectively) (Figure 5B; Movies S1–S3). Unlike a previous report that MDP25 greatly increased the disassembled rate of the microtubule plus-end *in vitro* (Li et al., 2011), we did not observe a significant difference in shrinkage rate of the microtubule plus-end between *mdp25* or OE and WT cells (Figure 5B). This could be due to the complexity of plant cells. The catastrophe frequency, rescue frequency, and shrinkage rate of individual microtubules increased while the time in pause phase decreased under salt treatment compared with control conditions, suggesting that the plus-end of microtubules in cells exposed to salt was prone to dynamic instability. The catastrophe and rescue frequencies of microtubules in WT cells increased by 80.4% and 47.5%, respectively, and those in OE cells increased by 67.9% and 41.9%, respectively, under salt treatment compared with control conditions. Although these two parameters in *mdp25* cells increased by 104.7% and 28.3%, respectively, under salt treatment compared with control conditions, the parameter values were only 0.0048/sec and 0.0044/sec under salt treatment, respectively. The shrinkage rate of individual microtubules in *mdp25* cells increased by 6.5% and time in pause phase reduced by 15.5% under salt treatment compared with control conditions, which were much smaller changes than those in WT cells (26.9% increase in shrinkage rate and 36.0% decrease in time in pause phase) or in OE cells (13.2% increase in shrinkage rate and 45.7% decrease in pause phase) (Figure 5B; Movies S4–S6). These data demonstrate that MDP25 plays an important role in regulating the dynamics of the microtubule plus-end under salt treatment.

In addition to the disassembly of microtubules at the plus-end, MDP25 can also increase the depolymerization rate at the minus-end *in vitro* (Li et al., 2011). However, research on the dynamics of individual microtubules at the minus-end is sparse. Therefore, we investigated whether MDP25 affects the dynamics of microtubule minus-end under salt treatment by analyzing cortical microtubules with a clearly visible minus-end in NaCl-treated WT, *mdp25*, and OE seedlings (Figure 6A). The minus-end of individual microtubules was continuously depolymerized *in vivo*. Consistent with a previous finding that MDP25 promotes the depolymerization of the microtubule minus-end *in vitro* (Li et al., 2011), the depolymerization rate was faster in OE cells and slower in *mdp25* cells (133.1% and 85.8% that in WT cells, respectively) under control conditions (Figure 6B; Movies S7–S9). These results suggest that MDP25 also regulates the depolymerization of microtubules at the minus-end *in vivo*. Under salt treatment, the depolymerization rate at the microtubule minus-end in WT cells increased by 46.7% compared with the control treatment (Figure 6B; Movie S10), suggesting that depolymerization at the microtubule minus-end accelerates under salt treatment. The depolymerization rate at the microtubule minus-end in OE cells (Movie S12) was still higher than that in WT cells under salt treatment, whereas there was no significant change in the depolymerization rate of individual microtubules at the minus-end in *mdp25* cells with or without salt treatment (Figure 6B; Movie S11). These results demonstrate that MDP25 regulates microtubule dynamics at the minus-end during the plant response to salt treatment.

17447909, 2022, 6, Downloaded from https://onlinelibrary.wiley.com/doi/10.1111/jipb.13264 by Northwest Agri & Forestry, Wiley Online Library on [03/11/2026]. See the Terms and Conditions (https://onlinelibrary.wiley.com/terms-and-conditions) on Wiley Online Library for rules of use; OA articles are governed by the applicable Creative Commons License

A



B

Dynamic parameters		Growth rate (μm/min)	Shrinkage rate (μm/min)	Catastrophe (events/second)	Rescue (events/second)	Time in growth phase (%)	Time in pause phase (%)	Time in shrinkage phase (%)
CK	WT	3.70 ± 0.76	8.25 ± 2.41	0.0047 ± 0.0036	0.0038 ± 0.0027	62.0 ± 12.5	15.8 ± 9.9	22.1 ± 10.2
	mdp25	3.45 ± 1.07	8.29 ± 3.89	0.0023 ± 0.0026	0.0034 ± 0.0048	62.3 ± 18.4	16.2 ± 14.6	21.7 ± 14.1
	OE	2.79 ± 0.88	8.81 ± 3.57	0.0056 ± 0.0027	0.0040 ± 0.0038	61.5 ± 14.2	16.0 ± 15.1	22.5 ± 9.3
Salt	WT	3.23 ± 0.88**	10.47 ± 3.57*	0.0085 ± 0.0106**	0.0056 ± 0.0059**	64.9 ± 15.3	9.3 ± 11.2*	25.8 ± 12.0
	mdp25	3.58 ± 0.99	8.83 ± 3.43	0.0048 ± 0.0044**	0.0044 ± 0.0039*	65.0 ± 14.9	13.7 ± 12.4	21.1 ± 11.3
	OE	2.84 ± 0.88	10.98 ± 2.90**	0.0088 ± 0.0039**	0.0055 ± 0.0043*	64.7 ± 15.8	8.7 ± 10.9*	27.6 ± 15.1

Figure 5. MDP25 affects the dynamics of the microtubule plus-end

(**A**) Time-lapse images showing the microtubule dynamics at the plus-end of a representative microtubule (labeled with red dots). The yellow arrow indicates the position of the microtubule plus-end. Bar = 5 μm. (**B**) The dynamic parameters at the plus-end of individual microtubules in hypocotyl cells from wild-type (WT), *mdp25*, or *MDP25*-overexpressing (OE) seedlings grown under 150 mmol/L NaCl treatment. More than 50 microtubules with a clearly visible leading plus-end from 20 cells of each sample condition were scored. $^{*}P < 0.05$ and $^{**}P < 0.01$ by *t*-test compared with the dynamic parameters in the same genotype under CK conditions. Data represent means ± *SD*. CK, control conditions; MDP25, MICROTUBULE-DESTABILIZING PROTEIN 25.

DISCUSSION

Our results show that MDP25 decodes the Ca^{2+} signal, a core signal in the salt signaling pathway, by changing its subcellular localization under salt stress. Moreover, MDP25 regulates microtubule organization by affecting the dynamics of individual microtubules at both the plus- and minus-ends, thus affecting plant seedling survival under salt stress.

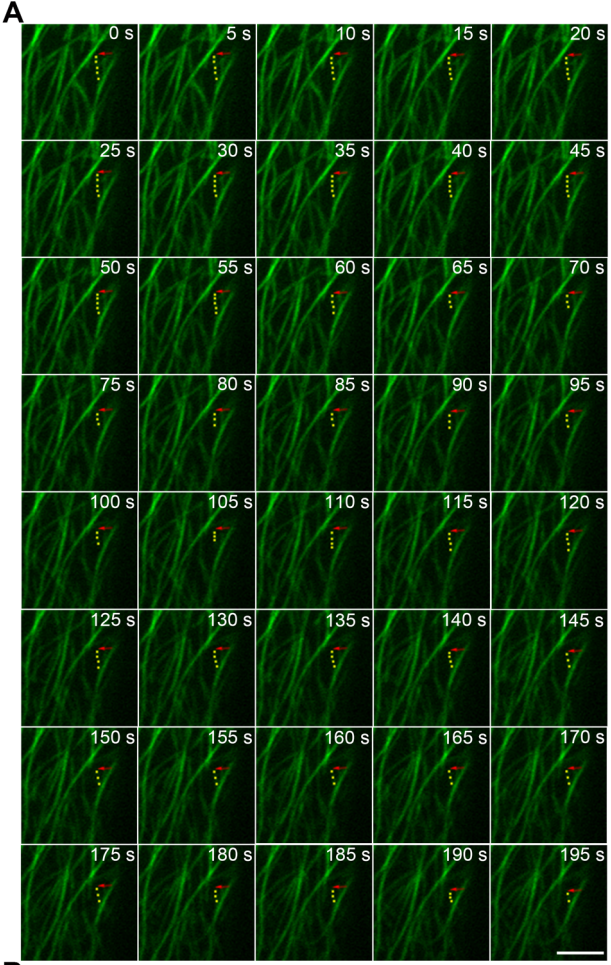
MDP25 regulates microtubule reorganization under salt stress

Microtubules play essential roles in plant responses to salt stress (Nick, 2013; Zhang and Zhang, 2016; Angelini et al., 2018). Salt stress causes ionic stress that results in microtubule depolymerization (Shoji et al., 2006), and under prolonged exposure, microtubules undergo rapid depolymerization followed by reassembly to form a new microtubule network. A low dosage of the microtubule-disrupting reagent oryzalin (0.1 μmol/L) promotes the biphasic reorganization of cortical microtubules and plant survival by facilitating the original depolymerization of microtubules, and a 4-μmol/L dosage of the microtubule-stabilizing reagent taxol disrupts biphasic reorganization and plant survival under salt stress (Wang et al., 2007). These observations indicate the importance of the biphasic reorganization of microtubules for plant survival under high-salinity conditions. MAPs play important roles in regulating this process. Upon exposure to salt stress, degradation of SPR1 promotes microtubule depolymerization (Wang et al., 2011). Increased expression of *WDL5* and activity of MAP65-1 and CC1, as well as the sequestration of RIC1, facilitate microtubule reassembly (Zhang et al., 2012; Li et al., 2017; Dou et al., 2018; Kesten et al., 2019). However, the mechanisms underlying the precise regulation of biphasic microtubule reorganization are still largely unknown.

The findings of this study support the idea that MDP25 plays a role in the regulation of microtubule reorganization under salt stress. Upon salt stress, cortical microtubules depolymerize rapidly, which is promoted by MDP25. Deficiency of *MDP25* in *mdp25* seedlings disrupted the depolymerization of microtubules, and OE of *MDP25* in OE seedlings promoted this process. Although silencing of *MDP25* reduced depolymerization efficiency, most microtubules in *mdp25* cells were depolymerized within 4 h, suggesting that other proteins, such as SPR1 or Propyzamide-Hypersensitive 1, which regulate microtubule depolymerization under salt stress (Wang et al., 2011; Fujita et al., 2013), likely co-regulated this process with MDP25. In the absence of

17447909, 2022, 6, Downloaded from https://onlinelibrary.wiley.com/doi/10.1111/jipb.13264 by Northwest Agri & Forestry, Wiley Online Library on [03/11/2026]. See the Terms and Conditions (https://onlinelibrary.wiley.com/terms-and-conditions) on Wiley Online Library for rules of use; OA articles are governed by the applicable Creative Commons License

A



B

Depolymerization rate (μm/min)	WT	*mdp25*	OE
CK	0.467 ± 0.083	0.401 ± 0.168	0.622 ± 0.098
Salt	0.685 ± 0.213**	0.419 ± 0.108*	0.839 ± 0.136**

Figure 6. MDP25 affects the depolymerization rate of the microtubule minus-end

(**A**) Time-lapse images showing the depolymerization process at the minus-end of a representative microtubule (labeled with yellow dots). The red arrow indicates the position of the microtubule minus-end. Bar = 5 μm. (**B**) The depolymerization rate of the microtubule minus-end in hypocotyl cells from wild-type (WT), *mdp25*, or *MDP25*-overexpressing (OE) seedlings grown under 150 mmol/L NaCl treatment. More than 50 microtubules with a clearly visible minus-end from 20 cells of each sample conditions were scored. $^{*}P < 0.05$ and $^{**}P < 0.01$ by *t*-test compared with the depolymerization rate in the same genotype under CK conditions. Data represent means ± *SD*. CK, control conditions; MDP25, MICROTUBULE-DESTABILIZING PROTEIN 25.

MDP25, other proteins play an alternative role in the *mdp25* mutant.

The dynamics of individual microtubules at the plus-end have a pivotal role in microtubule reorganization under salt stress (Endler et al., 2015; Li et al., 2017). Our results showed that, under salt treatment, the catastrophe and rescue frequencies and the shrinkage rate increased notably, whereas the time in pause phase shortened compared with under control conditions, indicating that the plus-end of individual microtubules are unstable under salt treatment. Moreover, under salt stress, the catastrophe and rescue frequencies and the shrinkage rate at the plus-end of individual microtubules in WT and OE cells increased to levels much higher than those in *mdp25* cells, while the time in pause phase was much longer in *mdp25* than in WT or OE cells. These findings suggest that MDP25 promotes microtubule plus-end instability under salt treatment.

The depolymerization rate at the minus-end of individual microtubules, which could be promoted by MDP25 *in vitro* (Li et al., 2011), increased significantly under salt stress compared with control conditions. Compared with that in WT cells, the depolymerization rate was lower in *mdp25* but higher in OE cells under salt treatment, suggesting that MDP25 promoted the depolymerization of the microtubule minus-end under salt treatment. These data demonstrate that MDP25 facilitated microtubule disassembly upon salt stress by affecting microtubule dynamics at both the plus- and minus-ends.

The reassembly of cortical microtubules was delayed in OE cells, while the knockout of *MDP25* led to faster reassembly, suggesting that artificially maintaining high expression levels of *MDP25* after microtubule depolymerization is unfavorable for the reassembly of microtubules. The expression of *MDP25* increased slightly after exposure to salt for 18 h, which could be due to a compensation effect for the reduction of *MDP25* expression at 6 h. Another possible explanation for this odd phenomenon is that a slight increase in *MDP25* expression may not result in a significant increase of protein function since MDP25 activity is affected by Ca^{2+} signaling under salt stress. Consistent with this idea, the higher *MDP25* expression at 18 h did not cause an increase in depolymerization of microtubules.

The results of a long-term observational study showed that cortical microtubules depolymerize again after reassembly under salt stress (Li et al., 2017). Knockout of *MDP25* facilitated the maintenance of microtubule integrity under prolonged exposure to salt for 48 h and the recovery of microtubules when salt stress was removed. However, artificially maintaining higher expression levels of *MDP25* was unfavorable for those processes. Consistent with this observation, more *mdp25* seedlings but fewer OE seedlings survived under salt stress. The microtubule-disrupting reagent oryzalin improved the resistance of WT seedlings to salt stress, but reduced OE seedling survival. By contrast, the microtubule-stabilizing reagent paclitaxel reduced the tolerance of seedlings to salt stress, but the effect on OE seedlings was very weak. These data demonstrate that the effect of MDP25 on microtubule organization under salt treatment could be one of the mechanisms by which MDP25 regulates plant responses to salt stress.

MDP25 can bind to PtdInsPs in the plasma membrane, and it is thought that PtdInsPs function as a signaling complex (Kato et al., 2010, 2019). MDP25 also has an actin filament-severing activity, and it regulates pollen tube growth

17447909, 2022, 6, Downloaded from https://onlinelibrary.wiley.com/doi/10.1111/jipb.13264 by Northwest Agri & Forestry, Wiley Online Library on [03/11/2026]. See the Terms and Conditions (https://onlinelibrary.wiley.com/terms-and-conditions) on Wiley Online Library for rules of use; OA articles are governed by the applicable Creative Commons License

and potyvirus filamentous particle cell-to-cell movement by modulating actin filaments (Qin et al., 2014; Cheng et al., 2020). Treatment of seedlings with 10 nmol/L of the F-actin depolymerization reagent LatB significantly increased the proportion of dead OE seedlings, suggesting that MDP25-mediated actin dynamics might be related to its function in plant adaptations to salt stress. However, it is still unclear whether the effects of MDP25 on PtdInsPs and actin filaments are involved in plant responses to salt stress and what the underlying mechanisms might be. These are interesting topics for future research.

MDP25 decodes the Ca^{2+} signal in the salt pathway

Although a cytosolic salt imbalance in plants leads to microtubule depolymerization, NaCl does not affect microtubule status *in vitro*, even when the salt concentration is as high as 400 mmol/L (Shoji et al., 2006), suggesting that NaCl itself is not a direct regulator of microtubules. Therefore, clarifying the signaling pathway from sensing Na^+ to microtubules is important for understanding the regulatory mechanism of microtubules under salt stress. Recently, several upstream processes related to MAPs that are involved in microtubule reorganization under salt stress have been identified, such as the degradation of SPR1 by the 26S proteasome, the regulation of MAP65-1 by PA, the sequestering of RIC1 by ROP2 and the transcription regulation of *WDL5* by ethylene-insensitive3 (Wang et al., 2011; Zhang et al., 2012; Li et al., 2017; Dou et al., 2018). However, the direct connections between the salt signaling pathways, especially the core signals, and microtubules remain unknown.

Here, we demonstrated that MDP25 is a junction between core salt signaling and microtubule organization. Glycosyl inositol phosphorylceramide sphingolipid (GIPC) acts as a possible Na^+ receptor for sensing Na^+ in the apoplastic space and activating Ca^{2+} influx channels in plants (Jiang et al., 2019). The hyperosmolality-gated calcium-permeable channel reduced hyperosmolality-induced $[Ca^{2+}]i$ Increase 1 (OSCA1) senses the osmotic stress induced by salt and elevates cytosolic Ca^{2+} concentration (Yuan et al., 2014). MDP25 mainly localizes to the plasma membrane under physiological concentrations of Ca^{2+}. Increased Ca^{2+} levels cause MDP25 to partially dissociate from the plasma membrane and move into the cytoplasm (Nagasaki et al., 2008; Li et al., 2011; Qin et al., 2014). Previous studies demonstrated that NaCl or KCl did not release MDP25 from membranes *in vitro* (Ide et al., 2007). Our data showed that MDP25 partially dissociated from the plasma membrane under NaCl treatment, and this relocation could be inhibited by the Ca^{2+} chelator BAPTA-AM, suggesting that elevation of Ca^{2+} stimulated by salt stress was the reason for MDP25 dissociation from the plasma membrane. Furthermore, Ca^{2+} enhances the microtubule-destabilizing activity of MDP25 (Qin et al., 2012). MDP25 dissociated from the plasma membrane within 20 min, and the microtubules were partially depolymerized in WT cells within 0.5 h under salt treatment. When the elevation of cytosolic Ca^{2+} was disrupted by the calcium chelator BAPTA-AM or calcium-channel blocker $LaCl_3$, the depolymerization of microtubules in WT and OE cells was much slower, while there was no obvious effect on *mdp25* cells. These results demonstrate that the Ca^{2+} signal in the salt pathway regulates the effect of MDP25 on microtubules by causing it to partially dissociate from the plasma membrane and enhancing its microtubule-destabilizing activity.

Therefore, we established a connection between the salt signaling pathway and microtubule organization. Under non-stress conditions, MDP25 localizes to the plasma membrane. When plants encounter salt stress, cytosolic Ca^{2+} concentration is elevated by GIPC or OSCA1. MDP25 decodes the Ca^{2+} signal and partially dissociates from the plasma membrane into the cytoplasm; Ca^{2+}-bound MDP25 also has a high microtubule-destabilizing activity. Microtubule instability increases due to the dynamics of individual microtubules, such as the catastrophe and rescue frequencies, shrinkage rate and time in pause phase at the microtubule plus-end and the depolymerization rate at the microtubule minus-end. This promotes microtubule depolymerization (Figure 7). After microtubule depolymerization, the expression of *MDP25* decreases, which probably facilitates microtubule reassembly. Therefore, this work establishes a connection between the core salt signaling pathway and microtubule organization.

MATERIALS AND METHODS

Plant materials and growth conditions

The *Arabidopsis mdp25* mutant (SAIL_241_A08), P_{MDP25}:*GUS*, *35S:MDP25-GFP*, P_{MDP25}:*MDP25-GFP/mdp25*, and P_{MDP25}:*mMDP25-GFP/mdp25*, as well as the WT, *mdp25*, and OE seedlings with YFP-tubulin tags, have been previously described (Li et al., 2011; Qin et al., 2014). Seeds were sterilized with 50% bleach in 0.01% Triton X-100 solution and placed on 1/2 MS medium (Sigma-Aldrich) plates containing 1% agar and 1% sucrose. After stratification at 4° C for 3 d, plates were placed in a growth chamber (22°C with a 16-h light/8-h dark cycle) for germination and growth. One-week-old seedlings were transferred to soil and grown in a growth room at 22°C with a 16-h light/8-h dark cycle.

β-glucuronidase staining

Seven-d-old P_{MDP25}:*GUS* transgenic seedlings were immersed in 1/2 MS solution with 175 mmol/L NaCl for 0, 6, 12, 18, 24, or 30 h. Samples were immersed in GUS staining buffer (0.1 mol/L phosphate buffer pH 7.0, 1 mmol/L ethylenediaminetetraacetic acid pH 8.8, 0.5 mmol/L potassium ferricyanide, 0.5 mmol/L potassium ferrocyanide, 1 mmol/L X-gluc, 1% (v/v) Triton X-100) at 37°C overnight. The samples were de-stained with 70% ethanol and 30% acetic acid.

Real-time PCR

Seven-d-old WT seedlings grown on 1/2 MS medium plates were immersed in 1/2 MS solution with or without 175 mmol/L NaCl for 0, 6, 12, 18, 24, or 30 h. Total RNA was extracted using a Plant RNeasy Kit (Qiagen). Complementary DNAs

17447909, 2022, 6, Downloaded from https://onlinelibrary.wiley.com/doi/10.1111/jipb.13264 by Northwest Agri & Forestry, Wiley Online Library on [03/11/2026]. See the Terms and Conditions (https://onlinelibrary.wiley.com/terms-and-conditions) on Wiley Online Library for rules of use; OA articles are governed by the applicable Creative Commons License

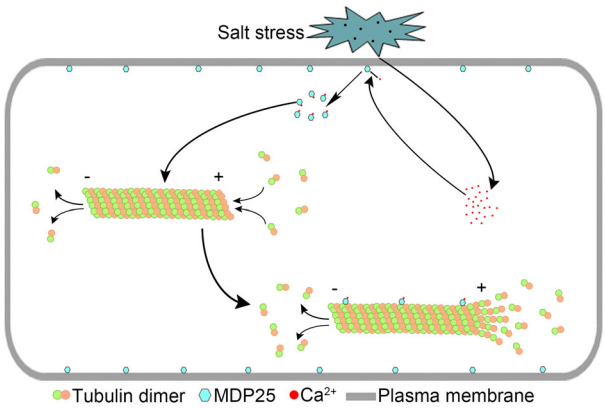


Figure 7. Model of MDP25 function in the regulation of microtubule depolymerization under salt stress

Under non-stress conditions, MDP25 localizes to the plasma membrane. Upon salt stress, cytosolic Ca^{2+} concentration is elevated. MDP25 decodes the Ca^{2+} signal and partially dissociates from the plasma membrane into the cytoplasm. Ca^{2+}-bound MDP25 also has a higher microtubule-destabilizing activity. Therefore, microtubule depolymerization is promoted by regulating the parameters of individual microtubules at both the plus- and minus-ends, such as the catastrophe and rescue frequencies, shrinkage rate and time in pause phase at the plus-end and the depolymerization rate at the minus-end. MDP25, MICROTUBULE-DESTABILIZING PROTEIN 25

(cDNAs) were synthesized using Superscript II Reverse Transcriptase (Takara). Real-time PCR was performed on an ABI 7900HT Fast Real-Time PCR System using SYBR Green PCR Master Mix (Applied Biosystems). The primers used for *MDP25* were 5′-CGCAGGACCGGTCACGTTCA-3′ and 5′-TTCAGCCACTGGCGCTGTCG-3′. 18S ribosomal RNA (rRNA) (5′-CGGCTACCACATCCAAGGAA-3′ and 5′-GCTGGAATTACCGCGCGGCT-3′) was used as an internal control. Error bars represent *SD* from three biological replicates.

Subcellular localization observation

The subcellular localization of MDP25 under salt treatment was observed by immersing 5-d-old *35S:MDP25-GFP* transgenic seedlings in distilled water with or without 175 mmol/L NaCl for 0, 20, or 40 min. Alternatively, *35S:MDP25-GFP* transgenic seedlings were immersed in 300 μmol/L BAPTA-AM (Sigma) solution for 30 min and treated with distilled water with or without 175 mmol/L NaCl in the presence of 300 μmol/L BAPTA-AM. The localization of MDP25 in epidermal cells of hypocotyls was visualized using a Zeiss 900 confocal microscope.

To observe the subcellular localization of MDP25 and mMDP25, 5-d-old P_{MDP25}:*MDP25-GFP/mdp25* and P_{MDP25}:*mMDP25-GFP/mdp25* transgenic plants were treated with 175 mmol/L NaCl for 40 min. The localization of MDP25 or mMDP25 in epidermal cells at the bottom of hypocotyls were visualized using a Zeiss 900 confocal microscope.

Salt stress treatment

To analyze seedling growth under salt treatment, 4-d-old WT, *mdp25*, OE, or P_{MDP25}:*MDP25/mdp25* transgenic seedlings grown on 1/2 MS medium plates were transferred onto 1/2 MS plates supplemented with 0, 150, or 175 mmol/L NaCl. Seven d later, the proportion of dead seedlings was determined. For NaCl treatment of soil-grown seedlings, 4-week-old WT, *mdp25*, OE, or P_{MDP25}:*MDP25/mdp25* transgenic seedlings were irrigated with 175 mmol/L NaCl. Photographs were taken before and after salt treatment for 8 and 15 d, respectively.

To analyze the effect of the microtubule-disrupting reagent oryzalin or the microtubule-stabilizing reagent paclitaxel on seedling survival under salt treatment, 4-d-old WT, *mdp25* and OE seedlings grown on 1/2 MS medium plates were transferred onto 1/2 MS plates supplemented with 175 mmol/L NaCl alone, or with 175 mmol/L NaCl and 0.5 μmol/L oryzalin (Sigma) or 2 μmol/L paclitaxel (Taxol; Sigma). Seven d later, the proportion of dead seedlings was determined. To analyze the effect of the F-actin depolymerization reagent LatB on seedling survival under salt treatment, 4-d-old WT, *mdp25* and OE seedlings grown on 1/2 MS medium plates were transferred onto 1/2 MS plates supplemented with 175 mmol/L NaCl and 0 or 10 nmol/L LatB (Sigma). Seven d later, the proportion of dead seedlings was determined.

Observation and quantification of cortical microtubules

For observation of the microtubule biphasic reorganization under salt treatment, 5-d-old WT, *mdp25*, and OE seedlings with YFP-tubulin tags grown on 1/2 MS medium plates were immersed in 1/2 MS solution with 175 mmol/L NaCl for 0, 0.5, 1, 2, 4, 8, 12, 18, 24, 32, or 48 h. The cortical microtubules in epidermal cells from the hypocotyl upper region were observed using a Zeiss 900 confocal microscope. To analyze the effect of BAPTA-AM or $LaCl_3$ on the depolymerization of microtubules under salt treatment, 5-d-old WT, *mdp25*, and OE seedlings with YFP-tubulin tags were immersed in 1/2 MS solution supplemented with 300 μmol/L BAPTA-AM or 2 μmol/L $LaCl_3$ for 30 min and then treated with 175 mmol/L NaCl in the presence of 300 μmol/L BAPTA-AM or 2 μmol/L $LaCl_3$ for 0, 1, 2, or 4 h. The cortical microtubules in epidermal cells from the hypocotyl upper region were analyzed. For the recovery of depolymerized microtubule organization after removal of the salt stress, 5-d-old WT, *mdp25*, and OE seedlings with YFP-tubulin tags grown on 1/2 MS medium plates were transferred onto 1/2 MS medium plates supplemented with 200 mmol/L NaCl for 3 d. The seedlings were transferred back onto 1/2 MS medium plates for cortical microtubule recovery. The cortical microtubules in hypocotyl or pavement cells were observed at 2 and 3 d after being transferred onto NaCl medium plates and 1 and 2 d after being transferred back onto 1/2 MS media.

The microtubule quantification was performed as previously described (Li et al., 2017; Dou et al., 2018). A vertical line perpendicular to the majority of the cortical microtubules was drawn and the number of cortical microtubules crossing the line was quantified using ImageJ software (http://rsb.info.nih.gov/ij/). The microtubule density was defined as the

17447909, 2022, 6, Downloaded from https://onlinelibrary.wiley.com/doi/10.1111/jipb.13264 by Northwest Agri & Forestry, Wiley Online Library on [03/11/2026]. See the Terms and Conditions (https://onlinelibrary.wiley.com/terms-and-conditions) on Wiley Online Library for rules of use; OA articles are governed by the applicable Creative Commons License

number of cortical microtubules per 10 μm. Measurements were performed in triplicate for each cell, and more than 20 cells per treatment were used.

Measurement of individual microtubule dynamics

Five-d-old WT, *mdp25*, and OE seedlings with YFP-tubulin tags were immersed in 1/2 MS solution with or without 150 mmol/L NaCl for 1 h. Time-lapse images of microtubules in hypocotyl cells were captured every 5 s for 5 min under a spinning disc confocal microscope with an Andor iXon charge-coupled device camera. Microtubule dynamic parameters were calculated using ImageJ software as previously described (DeBolt et al., 2007; Liu et al., 2013). Microtubules with a visible plus- or minus-end that could be tracked over 20 successive frames were used for the calculations. More than 50 microtubules from 20 seedlings of each sample condition were scored. Rescue and catastrophe frequencies were measured and analyzed according to a previous description (Kirik et al., 2012). The catastrophe frequency was defined as the frequency of transitions from growth to shrinkage; the rescue frequency was defined as the frequency of transitions from shrinkage to growth.

Accession number

The accession number of the *MDP25* gene described in this article is At4g20260.

ACKNOWLEDGEMENTS

We thank Dr. Hua Zhao and Dr. Fengping Yuan (State Key Laboratory of Crop Stress Biology for Arid Areas, Northwest A&F University, Yangling, China) for confocal experimental assistance. This work was supported by the Northwest A&F University for scientific research start-ups (2452021101 to T.Q.), the Natural Science Basic Research Program of Shanxi Province (2021JQ-139 to T.Q.), and the National Natural Science Foundation of China (31872411 to T.H.).

CONFLICTS OF INTEREST

The authors declare no conflicts of interest.

AUTHOR CONTRIBUTIONS

T.Q. conceived the project idea. P.Y., J.J., J.Z., D.W., W.X., X.B., and X.Z. performed experiments and analyzed data. T. Q. wrote the manuscript. T.H., T.M., and T.Q. revised and edited the article. All authors read and approved of its content.

Edited by: Christopher J. Staiger, Purdue University, USA.

Received Nov. 25, 2021; **Accepted** Apr. 16, 2022; **Published** Apr. 18, 2022

OO: OnlineOpen

REFERENCES

Angelini, J., Vosolsobe, S., Skupa, P., Ho, A.Y.Y., Bellinvia, E., Valentova, O., and Marc, J. (2018). Phospholipase Ddelta assists to cortical microtubule recovery after salt stress. Protoplasma **255:** 1195–1204.

Britigan, B.E., Rasmussen, G.T., and Cox, C.D. (1998). Binding of iron and inhibition of iron-dependent oxidative cell injury by the "calcium chelator" 1,2-bis(2-aminophenoxy)ethane N,N,N′,N′-tetraacetic acid (BAPTA). Biochem. Pharm. **55:** 287–295.

Buschmann, H., and Lloyd, C.W. (2008). *Arabidopsis* mutants and the network of microtubule-associated functions. Mol. Plant **1:** 888–898.

Cheng, G., Yang, Z., Zhang, H., Zhang, J., and Xu, J. (2020). Remorin interacting with PCaP1 impairs *Turnip mosaic virus* intercellular movement but is antagonised by VPg. New Phytol. **225:** 2122–2139.

Choi, W.G., Toyota, M., Kim, S.H., Hilleary, R., and Gilroy, S. (2014). Salt stress-induced Ca^{2+} waves are associated with rapid, long-distance root-to-shoot signaling in plants. Proc. Natl. Acad. Sci. U.S.A. **111:** 6497–6502.

DeBolt, S., Gutierrez, R., Ehrhardt, D.W., Melo, C.V., Ross, L., Cutler, S. R., Somerville, C., and Bonetta, D. (2007). Morlin, an inhibitor of cortical microtubule dynamics and cellulose synthase movement. Proc. Natl. Acad. Sci. U.S.A. **104:** 5854–5859.

Deinlein, U., Stephan, A.B., Horie, T., Luo, W., Xu, G., and Schroeder, J.I. (2014). Plant salt-tolerance mechanisms. Trends Plant Sci. **19:** 371–379.

Dou, L., He, K., Higaki, T., Wang, X., and Mao, T. (2018). Ethylene signaling modulates cortical microtubule reassembly in response to salt stress. Plant Physiol. **176:** 2071–2081.

Dou, L., He, K., Peng, J., Wang, X., and Mao, T. (2021). The E3 ligase MREL57 modulates microtubule stability and stomatal closure in response to ABA. Nat. Commun. **12:** 2181.

Endler, A., Kesten, C., Schneider, R., Zhang, Y., Ivakov, A., Froehlich, A., Funke, N., and Persson, S. (2015). A mechanism for sustained cellulose synthesis during salt stress. Cell **162:** 1353–1364.

Fujita, S., Pytela, J., Hotta, T., Kato, T., Hamada, T., Akamatsu, R., Ishida, Y., Kutsuna, N., Hasezawa, S., Nomura, Y., Nakagami, H., and Hashimoto, T. (2013). An atypical tubulin kinase mediates stress-induced microtubule depolymerization in *Arabidopsis*. Curr. Biol. **23:** 1969–1978.

Gantet, P., Masson, F., Domergue, O., Marquis-Mention, M., Bauw, G., Inze, D., Rossignol, M., and de la Serve, B.T. (1996). Cloning of a cDNA encoding a developmentally regulated 22 kDa polypeptide from tobacco leaf plasma membrane. Biochem. Mol. Biol. Int. **40:** 469–477.

Giovannoni, M., Marti, L., Ferrari, S., Tanaka-Takada, N., Maeshima, M., Ott, T., De Lorenzo, G., and Mattei, B. (2021). The plasma membrane-associated Ca^{2+} -binding protein, PCaP1, is required for oligogalacturonide and flagellin-induced priming and immunity. Plant Cell Environ. **44:** 3078–3093.

Ide, Y., Nagasaki, N., Tomioka, R., Suito, M., Kamiya, T., and Maeshima, M. (2007). Molecular properties of a novel, hydrophilic cation-binding protein associated with the plasma membrane. J. Exp. Bot. **58:** 1173–1183.

Jiang, Z., Zhou, X., Tao, M., Yuan, F., Liu, L., Wu, F., Wu, X., Xiang, Y., Niu, Y., Liu, F., Li, C., Ye, R., Byeon, B., Xue, Y., Zhao, H., Wang, H.N., Crawford, B.M., Johnson, D.M., Hu, C., Pei, C., Zhou, W., Swift, G.B., Zhang, H., Vo-Dinh, T., Hu, Z., Siedow, J.N., and Pei, Z.M. (2019). Plant cell-surface GIPC sphingolipids sense salt to trigger Ca^{2+} influx. Nature **572:** 341–346.

Kato, M., Nagasaki-Takeuchi, N., Ide, Y., Tomioka, R., and Maeshima, M. (2010). PCaPs, possible regulators of PtdInsP signals on plasma membrane. Plant Signal. Behav. **5:** 848–850.

17447909, 2022, 6, Downloaded from https://onlinelibrary.wiley.com/doi/10.1111/jipb.13264 by Northwest Agri & Forestry, Wiley Online Library on [03/11/2026]. See the Terms and Conditions (https://onlinelibrary.wiley.com/terms-and-conditions) on Wiley Online Library for rules of use; OA articles are governed by the applicable Creative Commons License

Kato, M., Tsuge, T., Maeshima, M., and Aoyama, T. (2019). *Arabidopsis* PCaP2 modulates the phosphatidylinositol 4,5-bisphosphate signal on the plasma membrane and attenuates root hair elongation. Plant J. **99:** 610–625.

Kesten, C., Wallmann, A., Schneider, R., McFarlane, H.E., Diehl, A., Khan, G.A., van Rossum, B.J., Lampugnani, E.R., Szymanski, W.G., Cremer, N., Schmieder, P., Ford, K.L., Seiter, F., Heazlewood, J.L., Sanchez-Rodriguez, C., Oschkinat, H., and Persson, S. (2019). The companion of cellulose synthase 1 confers salt tolerance through a Tau-like mechanism in plants. Nat. Commun. **10:** 857.

Kirik, A., Ehrhardt, D.W., and Kirik, V. (2012). TONNEAU2/FASS regulates the geometry of microtubule nucleation and cortical array organization in interphase *Arabidopsis* cells. Plant Cell **24:** 1158–1170.

Landrein, B., and Hamant, O. (2013). How mechanical stress controls microtubule behavior and morphogenesis in plants: history, experiments and revisited theories. Plant J. **75:** 324–338.

Li, C., Lu, H., Li, W., Yuan, M., and Fu, Y. (2017). A ROP2-RIC1 pathway fine-tunes microtubule reorganization for salt tolerance in *Arabidopsis*. Plant Cell Environ. **40:** 1127–1142.

Li, J., Wang, X., Qin, T., Zhang, Y., Liu, X., Sun, J., Zhou, Y., Zhu, L., Zhang, Z., Yuan, M., and Mao, T. (2011). MDP25, a novel calcium regulatory protein, mediates hypocotyl cell elongation by destabilizing cortical microtubules in *Arabidopsis*. Plant Cell **23:** 4411–4427.

Liao, C., Zheng, Y., and Guo, Y. (2017). MYB30 transcription factor regulates oxidative and heat stress responses through ANNEXIN-mediated cytosolic calcium signaling in *Arabidopsis*. New Phytol. **216:** 163–177.

Liu, X., Qin, T., Ma, Q., Sun, J., Liu, Z., Yuan, M., and Mao, T. (2013). Light-regulated hypocotyl elongation involves proteasome-dependent degradation of the microtubule regulatory protein WDL3 in *Arabidopsis*. Plant Cell **25:** 1740–1755.

Nagasaki, N., Tomioka, R., and Maeshima, M. (2008). A hydrophilic cation-binding protein of *Arabidopsis thaliana*, AtPCaP1, is localized to plasma membrane via N-myristoylation and interacts with calmodulin and the phosphatidylinositol phosphates PtdIns(3,4,5)P(3) and PtdIns (3,5)P(2). FEBS J. **275:** 2267–2282.

Nagata, C., Miwa, C., Tanaka, N., Kato, M., Suito, M., Tsuchihira, A., Sato, Y., Segami, S., and Maeshima, M. (2016). A novel-type phosphatidylinositol phosphate-interactive, Ca-binding protein PCaP1 in *Arabidopsis thaliana*: stable association with plasma membrane and partial involvement in stomata closure. J. Plant Res. **129:** 539–550.

Nick, P. (2013). Microtubules, signalling and abiotic stress. Plant J. **75:** 309–323.

Pan, Z., Zhao, Y., Zheng, Y., Liu, J., Jiang, X., and Guo, Y. (2012). A high-throughput method for screening *Arabidopsis* mutants with disordered abiotic stress-induced calcium signal. J. Genet. Genomics **39:** 225–235.

Qin, T., Li, J., Yuan, M., and Mao, T. (2012). Characterization of the role of calcium in regulating the microtubule-destabilizing activity of MDP25. Plant Signal. Behav. **7:** 708–710.

Qin, T., Liu, X., Li, J., Sun, J., Song, L., and Mao, T. (2014). *Arabidopsis* microtubule-destabilizing protein 25 functions in pollen tube growth by severing actin filaments. Plant Cell **26:** 325–339.

Rodriguez-Milla, M.A., and Salinas, J. (2009). Prefoldins 3 and 5 play an essential role in *Arabidopsis* tolerance to salt stress. Mol. Plant **2:** 526–534.

Sampathkumar, A., Yan, A., Krupinski, P., and Meyerowitz, E.M. (2014). Physical forces regulate plant development and morphogenesis. Curr. Biol. **24:** R475–R483.

Sedbrook, J.C., and Kaloriti, D. (2008). Microtubules, MAPs and plant directional cell expansion. Trends Plant Sci. **13:** 303–310.

Shoji, T., Suzuki, K., Abe, T., Kaneko, Y., Shi, H., Zhu, J.K., Rus, A., Hasegawa, P.M., and Hashimoto, T. (2006). Salt stress affects cortical microtubule organization and helical growth in *Arabidopsis*. Plant Cell Physiol. **47:** 1158–1168.

Su, C., Klein, M.L., Hernandez-Reyes, C., Batzenschlager, M., Ditengou, F.A., Lace, B., Keller, J., Delaux, P.M., and Ott, T. (2020). The *Medicago truncatula* DREPP protein triggers microtubule fragmentation in membrane nanodomains during symbiotic infections. Plant Cell **32:** 1689–1702.

Tanaka-Takada, N., Kobayashi, A., Takahashi, H., Kamiya, T., Kinoshita, T., and Maeshima, M. (2019). Plasma membrane-associated Ca^{2+}-Binding protein PCaP1 is involved in root hydrotropism of *Arabidopsis thaliana*. Plant Cell Physiol. **60:** 1331–1341.

Vosolsobe, S., Petrasek, J., and Schwarzerova, K. (2017). Evolutionary plasticity of plasma membrane interaction in DREPP family proteins. Biochim. Biophys. Acta Biomembr. **1859:** 686–697.

Wang, C., Li, J., and Yuan, M. (2007). Salt tolerance requires cortical microtubule reorganization in *Arabidopsis*. Plant Cell Physiol. **48:** 1534–1547.

Wang, S., Kurepa, J., Hashimoto, T., and Smalle, J.A. (2011). Salt stress-induced disassembly of *Arabidopsis* cortical microtubule arrays involves 26S proteasome-dependent degradation of SPIRAL1. Plant Cell **23:** 3412–3427.

Wang, X., and Mao, T. (2019). Understanding the functions and mechanisms of plant cytoskeleton in response to environmental signals. Curr. Opin. Plant Biol. **52:** 86–96.

Yamada, N., Theerawitaya, C., Kageyama, H., Cha-um, S., and Takabe, T. (2015). Expression of developmentally regulated plasma membrane polypeptide (DREPP2) in rice root tip and interaction with Ca^{2+}/CaM complex and microtubule. Protoplasma **252:** 1519–1527.

Yang, J., An, B., Luo, H., He, C., and Wang, Q. (2019). AtKATANIN1 modulates microtubule depolymerization and reorganization in response to salt stress in *Arabidopsis*. Int. J. Mol. Sci. **21:** 138.

Yang, Y., and Guo, Y. (2018). Elucidating the molecular mechanisms mediating plant salt-stress responses. New Phytol. **217:** 523–539.

Yu, Z., Duan, X., Luo, L., Dai, S., Ding, Z., and Xia, G. (2020). How plant hormones mediate salt stress responses. Trends Plant Sci. **25:** 1117–1130.

Yuan, F., Yang, H., Xue, Y., Kong, D., Ye, R., Li, C., Zhang, J., Theprungsirikul, L., Shrift, T., Krichilsky, B., Johnson, D.M., Swift, G.B., He, Y., Siedow, J.N., and Pei, Z.M. (2014). OSCA1 mediates osmotic-stress-evoked Ca^{2+} increases vital for osmosensing in *Arabidopsis*. Nature **514:** 367–371.

Zhang, Q., Lin, F., Mao, T., Nie, J., Yan, M., Yuan, M., and Zhang, W. (2012). Phosphatidic acid regulates microtubule organization by interacting with MAP65-1 in response to salt stress in *Arabidopsis*. Plant Cell **24:** 4555–4576.

Zhang, Q., and Zhang, W. (2016). Regulation of developmental and environmental signaling by interaction between microtubules and membranes in plant cells. Protein Cell **7:** 81–88.

Zhou, S., Chen, Q., Sun, Y., and Li, Y. (2017). Histone H2B monoubiquitination regulates salt stress-induced microtubule depolymerization in *Arabidopsis*. Plant Cell Environ. **40:** 1512–1530.

SUPPORTING INFORMATION

Additional Supporting Information may be found online in the supporting information tab for this article: http://onlinelibrary.wiley.com/doi/10.1111/jipb.13264/suppinfo

Movie S1. Dynamics at the plus-end of individual microtubules in a wild-type (WT) cell under control conditions

Movie S2. Dynamics at the plus-end of individual microtubules in an *mdp25* cell under control conditions

Movie S3. Dynamics at the plus-end of individual microtubules in a MICROTUBULE-DESTABILIZING PROTEIN 25 (MDP25)-overexpressing cell under control conditions

17447909, 2022, 6, Downloaded from https://onlinelibrary.wiley.com/doi/10.1111/jipb.13264 by Northwest Agri & Forestry, Wiley Online Library on [03/11/2026]. See the Terms and Conditions (https://onlinelibrary.wiley.com/terms-and-conditions) on Wiley Online Library for rules of use; OA articles are governed by the applicable Creative Commons License

Movie S4. Dynamics at the plus-end of individual microtubules in a wild-type (WT) cell under salt treatment
Movie S5. Dynamics at the plus-end of individual microtubules in an *mdp25* cell under salt treatment
Movie S6. Dynamics at the plus-end of individual microtubules in a MICROTUBULE-DESTABILIZING PROTEIN 25 (MDP25)-overexpressing cell under salt treatment
Movie S7. Dynamics at the minus-end of individual microtubules in a wild-type (WT) cell under control conditions
Movie S8. Dynamics at the minus-end of individual microtubules in an *mdp25* cell under control conditions
Movie S9. Dynamics at the minus-end of individual microtubules in a MICROTUBULE-DESTABILIZING PROTEIN 25 (MDP25)-overexpressing cell under control conditions
Movie S10. Dynamics at the minus-end of individual microtubules in a wild-type (WT) cell under salt treatment
Movie S11. Dynamics at the minus-end of individual microtubules in an *mdp25* cell under salt treatment
Movie S12. Dynamics at the minus-end of individual microtubules in a MICROTUBULE-DESTABILIZING PROTEIN 25 (MDP25)-overexpressing cell under salt treatment
Figure S1. Subcellular localization of MICROTUBULE-DESTABILIZING PROTEIN 25 (MDP25) and mutated MDP25 (mMDP25) under salt treatment
Figure S2. $LaCl_3$ slowed the depolymerization of microtubules in wild-type (WT) and overexpression (OE) cells
Figure S3. MICROTUBULE-DESTABILIZING PROTEIN 25 (MDP25) hinders the recovery of depolymerized microtubules in pavement cells after the removal of salt stress
Figure S4. Morphology of wild-type (WT), *mdp25*, and overexpression (OE) pavement cells under salt treatment
Figure S5. Complementary analysis of MICROTUBULE-DESTABILIZING PROTEIN 25 (MDP25) in regulating plant growth and survival under salt stress
Figure S6. Effects of oryzalin and paclitaxel on plant survival under salt stress
Figure S7. Effects of latrunculin B (LatB) on plant survival under salt stress.

JIPB
Scan using WeChat with your smartphone to view JIPB online
Scan with iPhone or iPad to view JIPB online

17447909, 2022, 6, Downloaded from https://onlinelibrary.wiley.com/doi/10.1111/jipb.13264 by Northwest Agri & Forestry, Wiley Online Library on [03/11/2026]. See the Terms and Conditions (https://onlinelibrary.wiley.com/terms-and-conditions) on Wiley Online Library for rules of use; OA articles are governed by the applicable Creative Commons License